

Published in final edited form as:

*Diabetes*. 2007 February ; 56(2): 285–294. doi:10.2337/db06-0436.

## IGF-Binding Protein-2 Protects Against the Development of Obesity and Insulin Resistance

Stephen B. Wheatcroft<sup>1</sup>, Mark T. Kearney<sup>1</sup>, Ajay M. Shah<sup>2</sup>, Vivienne A. Ezzat<sup>2</sup>, John R. Miell<sup>2</sup>, Michael Mado<sup>3</sup>, Stephen C.R. Williams<sup>3</sup>, Will P. Cawthorn<sup>4</sup>, Gema Medina-Gomez<sup>4</sup>, Antonio Vidal-Puig<sup>4</sup>, Jaswinder K. Sethi<sup>4</sup>, and Paul A. Crossey<sup>5</sup>

<sup>1</sup>Diabetes and Cardiovascular Research in Leeds, The LIGHT Laboratories, University of Leeds, U.K.

<sup>2</sup>Cardiovascular Division, King's College London, U.K.

<sup>3</sup>Institute of Psychiatry, King's College London, U.K.

<sup>4</sup>Department of Clinical Biochemistry, University of Cambridge, Cambridge, U.K.

<sup>5</sup>School of Biomedical and Molecular Sciences, University of Surrey, U.K.

### Abstract

Proliferation of adipocyte precursors and their differentiation into mature adipocytes contributes to the development of obesity in mammals. IGF-I is a potent mitogen and important stimulus for adipocyte differentiation. The biological actions of IGFs are closely regulated by a family of IGF-binding proteins (IGFBPs), which exert predominantly inhibitory effects. IGFBP-2 is the principal binding protein secreted by differentiating white preadipocytes, suggesting a potential role in the development of obesity. We have generated transgenic mice overexpressing human IGFBP-2 under the control of its native promoter, and we show that overexpression of IGFBP-2 is associated with reduced susceptibility to obesity and improved insulin sensitivity. Whereas wild-type littermates developed glucose intolerance and increased blood pressure with aging, mice overexpressing IGFBP-2 were protected. Furthermore, when fed a high-fat/high-energy diet, IGFBP-2-overexpressing mice were resistant to the development of obesity and insulin resistance. This lean phenotype was associated with decreased leptin levels, increased glucose sensitivity, and lower blood pressure compared with wildtype animals consuming similar amounts of high-fat diet. Our *in vitro* data suggest a direct effect of IGFBP-2 preventing adipogenesis as indicated by the ability of recombinant IGFBP-2 to impair 3T3-L1 differentiation. These findings suggest an important, novel role for IGFBP-2 in obesity prevention.

---

Obesity is a major public health problem, affecting up to 30% of adults in the U.S. (1). It is associated with an increased risk of insulin resistance, type 2 diabetes, hypertension, and cardiovascular disease, and it significantly reduces life expectancy (2). The development of obesity involves the expansion of the adipose tissue at the expense of a combined process

involving proliferation and differentiation of new adipocytes and enlargement of older adipocytes (3,4). Data from in vitro and in vivo studies support a role for IGF-I in adipocyte differentiation and proliferation (5-9). The activity of IGF-I is regulated by a family of IGF-binding proteins (IGFBPs), which bind IGF-I with a greater affinity than that of its tyrosine kinase receptor (10,11). The principal action of the IGFBPs is thought to be to regulate access of IGF-I to target tissues and hence reduce IGF-I bioactivity (10,11).

Despite their structural homology, individual members of the IGFBP family may exert unique actions. We previously demonstrated that IGFBP-1 is involved in placental development, glucose counter-regulation, and vascular homeostasis (12-14). IGFBP-1 has been shown to inhibit IGF-I-mediated differentiation of preadipocytes in vitro (15), whereas in vivo, diet-induced obesity is prevented in IGFBP-1-overexpressing mice (16). The latter effect was, however, associated with a substantial deterioration in glucose tolerance (16), consistent with our findings that mice overexpressing IGFBP-1 develop age-related glucose intolerance (12).

IGFBP-2 is the second most abundant circulating IGFBP, but its physiological roles remain poorly understood. However, it has been shown to be the principal IGFBP secreted by white preadipocytes during adipogenesis (17), leading us to hypothesize that IGFBP-2 may play an important role in modulating the effects of IGF-I on adipocyte development associated with obesity. Of interest, serum concentrations of IGFBP-2 are reduced in obese humans (18), in keeping with the possibility that reduced IGFBP-2 levels are permissive for the development of obesity. Here, we report on the generation and metabolic characterization of a transgenic mouse model overexpressing the human IGFBP-2 gene under control of its native promoter. Our findings demonstrate that IGFBP-2 exerts a beneficial effect in preventing both age and diet-induced obesity and its associated complications.

## RESEARCH DESIGN AND METHODS

### Generation of transgenic mice

A 39-kb *NotI* fragment of the human IGFBP-2 cosmid clone chBP2:4 (19) was gel-purified and microinjected into the pronucleus of single-cell embryos of FVB/N mice. Microinjected embryos were transferred to the oviducts of pseudopregnant CD-1 females. Transgenic offspring were identified by Southern blot analysis of tail DNA. Animals positive for the transgene were mated with wild-type FVB/N mice to establish different transgenic lines. The offspring of these matings were genotyped by PCR analysis of tail lysates with a primer combination that specifically amplifies a region of the human IGFBP-2 gene spanning exon 2.

Two transgenic lines were identified for use in the experiments described here. Breeding colonies were established by crossing male heterozygous IGFBP-2-overexpressing mice with wild-type female FVB/N animals. Preliminary experiments revealed sexual dimorphism of the metabolic phenotype of IGFBP-2 transgenic mice, with more pronounced differences in female animals. Therefore female transgenic mice and matched wild-type littermates were used in all experiments described. All procedures were performed in accordance with U.K. Home Office regulations and were approved by our institution's

ethics committee. Expression and tissue distribution of human IGFBP-2 mRNA were assessed by Northern blot (12), using [ $\alpha$ - $^{32}$ P]dCTP-labeled human IGFBP-2 cDNA, and by RT-PCR using primers specific for human IGFBP-2 (forward, cctgtgcagcagcttctcgtgag; reverse, cccaggctggcac catgctcacctg). Circulating concentrations of IGFBPs were assessed by Western immunoblot analysis of serum proteins using equimolar amounts of  $^{125}$ I-labeled IGF-I and IGF-II (12).

### Experimental design

The experimental protocol was designed to test the hypothesis that overexpression of IGFBP-2 would influence the development of obesity. In the first series of experiments, the influence of IGFBP-2 overexpression on glucose regulation was assessed in 8-week-old and 4- to 6-month-old animals. More detailed experiments were carried out in 8- and 40-week-old mice to examine the effects of IGFBP-2 overexpression on age related obesity and metabolic phenotype. In the second series of studies, mice were fed a high-fat diet (Diet F3282; Bioserve, Frenchtown, NJ) or standard laboratory chow (Special Diet Services, Essex, U.K.) for 32 weeks from weaning to determine the influence of IGFBP-2 overexpression on the development of diet-induced obesity.

### Glucose and insulin/IGF tolerance tests

Blood was sampled from the lateral saphenous vein after an overnight fast and repeated 4 h after re-feeding. Glucose, insulin, and IGF-I tolerance tests were performed by blood sampling at intervals after the intraperitoneal injection of glucose (1 mg/g), human recombinant insulin (0.5 unit/kg; Actrapid; Novo Nordisk, Bagsvaerd, Denmark), or human recombinant IGF-I (0.2  $\mu$ g/g; GroPep, Adelaide, Australia) (14). Glucose concentrations were determined in whole blood by a portable meter (Hemacue, Sheffield, U.K.). Plasma insulin concentrations were determined by enzyme-linked immunosorbant assay (Ultrasensitive Rat Insulin ELISA; CrystalChem). Plasma free fatty acids and triglyceride concentrations were determined using colorimetric assays (Free Fatty Acids Half-Micro test, Roche, Mannheim, Germany, and Thermotrace, Victoria, Australia, respectively) (14). Leptin levels were measured using a commercially available enzyme-linked immunosorbant assay (Diagnostic Systems Laboratories, Webster, TX).

### Blood pressure

Systolic blood pressure was measured using tail-cuff plethysmography (XBP1000; Kent Scientific, Torrington, CT) in conscious mice (20). Measurements were made on 3 separate days, and the mean of six consecutive readings made on these days was calculated.

### Energy intake and body temperature

Energy intake was estimated by measuring food intake during a 7-day period, midway through the experimental diet period. Core body temperature was measured with a rectal temperature probe.

### Morphometric analysis

Body size and composition was determined after 32 weeks of feeding mice high-fat or chow diets. Body length was measured from the tip of the nose to the base of the tail.

Reproductive adipose tissue was carefully dissected free from the uterus, ovaries, and adnexae; mesenteric adipose tissue was teased away from the stomach, small intestine, and large intestine; and brown adipose tissue was dissected free from the inter-scapular and subscapular regions. Adipose tissues were blotted dry before immediate weighing.

### Magnetic resonance imaging

Animals were scanned postmortem after 32 weeks of feeding, and regional adiposity was determined by calculating the cross-sectional area of fat measured on a scan plane centered at the level of the kidneys. Perfused animals were maintained in a paraformaldehyde-filled tube to prevent drying out of the specimens over the course of the scanning session. Imaging was performed on a small animal, horizontal bore, 4.7T NMR system (Oxford Systems) controlled by a UNITY Inova-200 imaging console (Varian). A quadrature birdcage radiofrequency coil with 63-mm internal diameter (Varian) was used for signal transmission and reception. Raw-time domain data were Fourier transformed using custom software. The optimal imaging protocol was determined by the need for a high spatial resolution and an ex vivo distinction between fat and other tissues, and consisted of coronal T<sub>2</sub>-weighted (repetition time = 1,250 ms, echo time = 16 ms) spin echo scans with a 512 (2) matrix size, eight averages per phase encoding step, 60 contiguous 2-mm-thick slices at an in-plane spatial resolution of 273  $\mu\text{m}$ .

The body of the animals was masked from the surrounding fracture using the semi-automated region of interest tool in Xdispimage (David Plummer, University College, London, U.K.). At a slice level through the middle of both kidneys, all pixels were summed to yield a total body area. The fat content within this abdominal slice was nominally ascribed to all pixels exceeding 1 SD greater than the signal intensity of the left kidney.

### Adipocyte area

Samples of peri-gonadal adipose tissue were fixed in 10% formalin and embedded in paraffin. Multiple sections (separated by 100  $\mu\text{m}$  each) were obtained from each sample and stained with hematoxylin and eosin. Digital images of each section were acquired using a digital camera (Hamamatsu C4742-95) and microscope (Zeiss Axioscop 2), and cell areas were traced manually for at least 100 cells per field by an investigator blinded to the sample identity, using Openlab software (Improvision). Two fields from each of two sections from each adipose tissue depot were analyzed to derive the mean cell area per animal ( $n = 6$  animals per group).

### Culture and differentiation of 3T3-L1 preadipocytes

Two-day postconfluent 3T3-L1 preadipocytes were induced in differentiation medium (Dulbecco's modification of Eagle's medium, containing 10% cosmic calf serum [Hyclone], 50 units/ml penicillin, and 50  $\mu\text{g/ml}$  streptomycin). For induction cocktails of varying potency, differentiation medium was further supplemented with dexamethasone (1  $\mu\text{mol/l}$ ),

3-isobutyl-1-methylxanthine (0.5 mmol/l), and either insulin (1  $\mu$ mol/l) or hrIGF (10 nmol/l), as indicated. Treatment in the presence of IGFBP-2 was performed with induction cocktail that had been preincubated with rhIGFBP-2 (100 nmol/l) for 30 min at room temperature. After 2 days, the induction medium was replaced with differentiation medium supplemented with either insulin or IGF-I  $\pm$  IGFBP-2, for a further 2 days. Thereafter, all monolayers were maintained in nonsupplemented differentiation medium. Uninduced control cells were maintained in nonsupplemented differentiation medium throughout. On day 8, monolayers were either fixed and lipid droplet-stained with Oil red O (21) or processed for total RNA extraction using a RNeasy kit (Qiagen). RNA was then quantified, reverse transcribed, and used to perform Taqman real-time PCR for murine peroxisome proliferator-activated receptor  $\gamma$  (PPAR $\gamma$ ), aP2, and 18S as described previously (22). To exclude an IGF-independent effect of IGFBP-2 on 3T3-L1 cell differentiation, the above experiment was repeated with human Des(1–3)IGF-I, an analog of IGF-I lacking the N-terminal tripeptide Gly-ProGlu, which does not bind to IGFBPs.

### Statistics

Results are expressed as means  $\pm$  SE. Comparisons between groups were made by unpaired two-tailed Student's *t* test or repeated measures ANOVA, as appropriate.  $P < 0.05$  was considered statistically significant.

## RESULTS

Transgenic mice were generated after microinjection of the *NotI* fragment of human IGFBP-2 cosmid clone chBP2:4 (Fig. 1A). Two lines of transgenic mice (tg1 and tg2) were generated (Fig. 1B). Overexpression of IGFBP-2 was not associated with any gross morphogenic or developmental abnormalities. Human IGFBP-2 mRNA was detected in a variety of organs and tissues of IGFBP-2 mice, including adipose depots, but was undetectable in wildtype littermates (Fig. 1C and D). Total levels of circulating IGFBP-2 in fasting serum were 2.2-fold higher in IGFBP-2 mice than wild type ( $P < 0.05$ ) (Fig. 1E). Birth weight and early postnatal growth did not differ between wild-type and IGFBP-2 transgenic mice in either line.

### IGFBP-2 prevents age-induced insulin resistance

Blood glucose and plasma insulin levels were similar in wild-type and transgenic mice (tg1 and tg2) at 8 weeks of age. By 4–6 months of age, however, nonfasted blood glucose levels were significantly lower in transgenic mice than in controls (Table 1). This was not explained by differences in insulin levels, which were similar between groups.

We carried out a more detailed investigation of the effect of IGFBP-2 on age-related changes in glucose homeostasis in tg1 animals at 8 (young) and 40 (old) weeks of age. In wild-type mice, glucose tolerance declined with age, as evidenced by higher glucose levels in old compared with young mice after a glucose tolerance test (GTT) (Fig. 2A). Conversely, IGFBP-2-overexpressing mice were protected against this age-related decline in glucose tolerance (Fig. 2A). Fasting insulin levels were similar in young and old wild-type mice (Fig. 2B), whereas the insulin response to GTT was significantly greater in old mice (Fig. 2B). In

IGFBP-2–overexpressing mice, however, there was no significant increase in plasma insulin concentrations with aging either in the fasting state or after a carbohydrate challenge (Fig. 2B). The lack of age-related increase in blood glucose levels after a GTT challenge in IGFBP-2–overexpressing mice could not therefore be explained by a greater rise in plasma insulin responses. These findings are consistent with IGFBP-2–mediated protection against age-induced development of insulin resistance. This was confirmed in insulin tolerance tests, in which the hypoglycemic response to exogenous insulin was significantly greater in 40-week-old IGFBP-2 mice than wild type (Fig. 2C). In IGF-I tolerance tests, on the other hand, the hypoglycemic response to recombinant IGF-I was significantly attenuated in IGFBP-2 mice (Fig. 2D), consistent with IGFBP-2 blunting the metabolic effects of IGF-I. There were no significant differences between 40-week-old IGFBP-2-overexpressing and wild-type mice in fasting plasma triglycerides ( $1.5 \pm 0.2$  vs.  $1.6 \pm 0.2$  mmol/l) or free fatty acids ( $1.9 \pm 0.2$  vs.  $2.1 \pm 0.2$  mmol/l). Body weight of IGFBP-2 mice was similar to that of wild-type mice at 8 weeks ( $20.1 \pm 0.2$  vs.  $19.9 \pm 0.4$  g) and 40 weeks ( $26.1 \pm 0.6$  vs.  $25.8 \pm 0.5$  g) of age when fed standard chow.

### IGFBP-2 transgenic mice are resistant to diet-induced obesity and fatty liver

To explore the effect of IGFBP-2 on the development of diet-induced obesity and its metabolic consequences, paired groups of wild-type and tg1 transgenic mice received standard chow or a high-fat/highcalorie diet for 32 weeks from 8 weeks of age. Weight gain was similar in groups receiving standard chow (Fig. 3A). However, weight gain on the high-fat diet was markedly attenuated in transgenic mice compared with wild-type mice (Fig. 3B). Linear growth, measured as nose-rump length at 40 weeks of age, was similar in transgenic and wild-type mice on chow ( $100 \pm 1$  vs.  $99 \pm 2$  mm) and high-fat ( $101 \pm 1$  vs.  $102 \pm 1$  mm) diets. Mice fed standard chow had relatively small adipose tissue depots, with no significant difference in mass of major fat depots between wild-type and IGFBP-2 mice (Fig. 3C). Wild-type mice fed with high-fat diet markedly increased their fat depots, whereas IGFBP-2 transgenic mice remained lean (Fig. 3D). Solid organ weights were similar in wild-type and IGFBP-2 mice on chow and high-fat diets, with the exception of liver weight which was lower in high-fat–fed IGFBP-2 mice (Fig. 3F). Interestingly, whereas the livers of wild-type high-fat–fed mice had a macroscopic appearance compatible with increased fat content, this finding was absent in IGFBP-2 mice (not shown), suggesting that IGFBP-2 overexpression ameliorates hepatic steatosis associated with obesity.

Quantification of intra-abdominal fat using magnetic resonance imaging (MRI) was performed by analysis of fat area at the level of the kidneys (Fig. 4A and B). This approach confirmed a substantial reduction in adiposity of high-fat–fed IGFBP-2 mice. Furthermore, chow-fed IGFBP-2 mice also had less abdominal fat than chow-fed wild types (Fig. 4), providing a potential explanation for the blunting of age-induced insulin resistance in IGFBP-2 mice. Adipocyte size was also estimated by histological assessment of sections of periovarian fat (Fig. 4C). The increase in adipocyte size with high-fat feeding was blunted in IGFBP-2 mice (mean cell area  $2,800 \pm 300$  vs.  $5,900 \pm 180$   $\mu\text{m}^2$ ;  $P < 0.01$ ) (Fig. 4D). Moreover, fat cells were also smaller in 40-week-old IGFBP-2 mice than wild-type controls receiving chow diet ( $1,390 \pm 130$  vs.  $2,100 \pm 130$   $\mu\text{m}^2$ ;  $P = 0.02$ ) (Fig. 4C and D)

There were no significant differences in glucose and insulin levels between fasted wild-type and transgenic mice on either diet (Fig. 5A and B). However, blood glucose after a GTT was significantly lower in IGFBP-2 than wild-type mice on both types of diet (Fig. 5A). Furthermore, the relative increase in blood glucose level induced by a high-fat diet was blunted in IGFBP-2 compared with wild-type mice (Fig. 5A). The protective effect of IGFBP-2 on the development of glucose intolerance after high-fat feeding was confirmed in full GTTs (Fig. 5C and D). Plasma free fatty acids were similar in high-fat-fed wild-type and IGFBP-2 mice ( $1.4 \pm 0.2$  vs.  $1.5 \pm 0.1$  mmol/l), whereas plasma triglyceride levels were significantly lower in IGFBP-2 than wild-type mice after high-fat feeding ( $1.4 \pm 0.1$  vs.  $1.6 \pm 0.1$  mmol/l;  $P < 0.05$ ). Plasma leptin levels were not significantly different in wild-type and IGFBP-2 mice receiving chow diet ( $8.9 \pm 1.4$  vs.  $4.2 \pm 1.4$  ng/ml;  $P = 0.19$ ). High-fat feeding resulted in an increase in leptin levels in wild-type animals, which was significantly blunted in IGFBP-2 mice ( $54.2 \pm 5$  vs.  $14.9 \pm 4$  ng/ml;  $P < 0.05$ ). Interestingly, total energy intake, estimated from the mean mass of diet consumed per day, was not significantly different between IGFBP-2 and wildtype mice on either chow ( $191 \pm 9$  vs.  $209 \pm 9$  mg  $\cdot$  g<sup>-1</sup> body mass  $\cdot$  day<sup>-1</sup>;  $P = 0.2$ ) or high-fat ( $96 \pm 6$  vs.  $91 \pm 3$  mg  $\cdot$  g<sup>-1</sup> body mass  $\cdot$  day<sup>-1</sup>;  $P = 0.5$ ) diets. Although there was a trend toward increased core body temperature in transgenic mice, we could not establish significant differences between IGFBP-2 transgenic and wild-type mice on both chow ( $37.2 \pm 0.1$  vs.  $37.6 \pm 0.3^\circ\text{C}$ ;  $P = 0.26$ ) and high-fat ( $37.5 \pm 0.2$  vs.  $38.2 \pm 0.2^\circ\text{C}$ ;  $P = 0.09$ ) diets.

### **IGFBP-2 inhibits adipogenesis in 3T3-L1 adipocytes by suppressing IGF-I action**

To investigate whether IGFBP-2 could itself impair adipocyte development, 3T3-L1 preadipocytes were induced to differentiate in the presence of recombinant hIGFBP-2. This treatment significantly blunted adipogenesis that was induced either by serum-containing induction cocktail alone or that which was supplemented with hIGF-1 (10 nmol/l). This was evident by the reduced number of lipid-laden cells (Fig. 6A and B) and reduced expression of key adipogenic markers, PPAR $\gamma$  and aP2 (Fig. 6C). In contrast, adipocyte differentiation in the presence of high-dose insulin was unaffected by the presence of recombinant hIGFBP-2, consistent with insulin not binding to the IGFBPs (Fig. 6A–C). Similarly, hIGFBP-2 did not affect adipocyte differentiation in the presence of Des(1–3)IGF-I (Fig. 6D and E), suggesting that IGFBP-2 inhibits adipogenesis by modulating IGF-I activity rather than by a direct effect of the protein on adipocytes.

### **IGFBP-2 overexpression prevents age-related hypertension**

We also evaluated the effect of IGFBP-2 on blood pressure. Systolic blood pressure increased with aging in wild-type mice, but this was blunted in IGFBP-2-overexpressing mice (Fig. 7). Moreover, IGFBP-2-overexpressing mice at 40 weeks had lower systolic blood pressure than wild type. Blood pressure was also investigated in mice fed high-fat diet. Wild-type mice (40 weeks old) on a high-fat diet had a higher systolic blood pressure than similar aged chow-fed mice, whereas high-fat feeding had no effect on blood pressure in IGFBP-2 transgenic mice (Fig. 7).

## DISCUSSION

Obesity, through its associations with impaired regulation of carbohydrate metabolism, hypertension, and atherosclerotic cardiovascular disease, significantly reduces life expectancy (2). Adiposity in humans develops in response to positive energy balance by complementary mechanisms leading to increase in volume of existing fat cells and the proliferation and subsequent differentiation of adipocyte precursor cells present in established fat depots (23). The current epidemic of obesity in developed nations, with its implications for public health, emphasizes the importance of understanding the complex regulatory mechanisms implicated in obesity development.

We have shown here that overexpression of IGFBP-2 in mice protects against the development of obesity in response to dietary excess and prevents the development of glucose intolerance and hypertension associated with advancing age. Using complementary approaches of adipose depot mass estimation and MRI, we demonstrated reductions in regional fat depots in IGFBP-2–overexpressing mice. Importantly, IGFBP-2 overexpression led to a significant reduction in fat cell size in both chow-fed and high-fat-fed animals. These findings may have resulted from an inhibitory effect of IGFBP-2 on intracellular accumulation of triacylglycerol or by an inhibitory action of IGFBP-2 on IGF-I–mediated adipogenesis. The latter is supported by our observation that recombinant IGFBP-2 inhibits adipogenesis *in vitro*. In these studies, IGFBP-2 significantly blunted 3T3-L1 cell differentiation induced by induction cocktail alone (which contains IGF-I in serum), or that which was supplemented with IGF-I, in keeping with an inhibitory action of IGFBP-2 on IGF-I–mediated adipogenesis.

IGF-I is produced by virtually all mammalian tissues and is of crucial importance in regulating cell differentiation/proliferation by a combination of endocrine, autocrine, and paracrine effects (24). Differentiation of adipocyte precursors into mature adipocytes is accompanied by increased expression of IGF-I (25). The demonstration that IGF-I is an important stimulus for adipocyte differentiation in preadipocyte primary culture (8,9,26) and cell lines (5,6) suggests that manipulation of IGF-I activity could be a potential therapeutic maneuver to attenuate the development of obesity.

Mice with null mutations of the genes encoding IGF-I and its receptor either die at birth or are severely growth restricted (27), consistent with an essential role of IGF-I in postnatal development. In contrast, mice with targeted deletion of IGF-I expression in the liver exhibit normal growth and development, despite significantly reduced circulating IGF-I levels (28,29). These data highlight the importance of local IGF-I production in regulating cell differentiation/proliferation and support the concept that tissue-derived IGF binding proteins may represent a potential substrate with which to modify autocrine/paracrine IGF-I effects. Interestingly, reduced adiposity has been reported in mice with targeted inactivation of hepatic IGF-I expression, although it is uncertain whether this was attributable to reduced circulating IGF-I concentrations or to changes in growth hormone and leptin levels (30).

Although members of the IGFBP family exhibit structural homology, the actions of the individual binding proteins are distinct, and this may impart upon the IGF-I/IGFBP axis a



degree of functional and/or tissue specificity (31). In our model, mice with overexpression of human IGFBP-2 under the control of its native promoter were protected against obesity but exhibited normal postnatal weight gain, linear growth, and solid organ development. This contrasts with the growth-restricted phenotype of a previously reported transgenic mouse in which IGFBP-2 was overexpressed under control of the cytomegalovirus promoter (in which normal tissue distribution was not achieved) (32). Similarly, postnatal growth and fertility are restricted in transgenic mice overexpressing IGFBP-3 (33), IGFBP-5 (34), and IGFBP-6 (35). In our model, transgene expression is under control of the native human IGFBP-2 promoter, and one may speculate that the fact that IGFBP-2 is the predominant IGFBP secreted by adipocytes during differentiation (17) leads to a relative specificity of the inhibitory effect of IGFBP-2 to adipose tissues. Localization of the inhibitory effects of IGFBP-2 on IGF-I bioactivity to fat is consistent with our observed phenotype of reduced adiposity without growth restriction. Mice with targeted deletion of IGFBP-2 have previously been reported, but the only phenotypic changes apparent were alterations in spleen and liver size (36). Responses to nutritional energy excess and susceptibility to obesity were not studied in this model.

Reduced susceptibility to diet-induced obesity was a major finding of the current study. IGFBP-2 mice fed standard chow also had higher insulin sensitivity and lower blood pressure than wild-type littermates. Although we were unable to demonstrate a difference in mass of reproductive, mesenteric, or subscapular fat depots, MRI-derived abdominal adiposity and adipocyte size were significantly reduced in chow-fed IGFBP-2 mice compared with chow-fed controls. These findings suggest that IGFBP-2 prevents the development of obesity and its metabolic and cardiovascular sequelae even without the challenge of nutritional energy excess.

Our data indicate that IGFBP-2 prevents the development of obesity and associated complications through a direct inhibitory effect on white adipose tissue development. However, we speculate that in the absence of differences in food intake, the differences in fat accumulation between these two mouse models may be related to compensatory increases in thermogenesis as the trend toward increased body temperature may suggest. Detailed studies of basal metabolic rate will be necessary to explore this possibility in more detail. Alternatively, we cannot exclude effects in locomotor activity and/or compensatory effects in fuel oxidation as added factors contributing to the lean phenotype.

In this study, we demonstrated using an insulin tolerance test that IGFBP-2-overexpressing mice were protected from the age-related decline in insulin sensitivity seen in wild-type animals. A euglycemic-hyperinsulinemic clamp study could be considered in the future to explore these findings in more detail. The favorable metabolic and cardiovascular phenotype of the IGFBP-2 mice may be attributable to changes in IGF-I bioavailability or may be secondary to reduced global adiposity and/or adipocyte size. Adipocytes secrete a range of circulating cytokines and peptides (including tumor necrosis factor- $\alpha$ , leptin, adiponectin, and resistin), that exert wide-ranging influences on metabolic and cardiovascular homeostasis (37,38). A favorable secretory profile of smaller adipocytes in IGFBP-2 mice, leading to reduced circulating leptin levels and increased adiponectin levels, for example, may at least partly explain the improvements in carbohydrate metabolism and blood

pressure when compared with wild-type littermates. We cannot exclude the possibility that other novel actions of IGFBP-2 contributed to the improved insulin sensitivity in IGFBP-2 mice through, for example, direct effects on fatty acid oxidation and energy dissipation. Future experiments will elucidate how IGFBP-2 promotes insulin sensitivity. In conclusion, these data highlight a novel function of IGFBP-2 in adipocyte biology and support an important role for IGFBP-2 in protecting against the development of obesity- and age-associated complications.

## ACKNOWLEDGMENTS

This work was funded by the British Heart Foundation (BHF), Diabetes U.K., Medical Research Council (MRC), Biotechnology and Biological Sciences Research Council (BBSRC), and Wellcome Trust. S.B.W. held a BHF Clinical PhD Studentship. M.T.K. held a BHF Intermediate Fellowship. A.M.S. holds a BHF Chair in Cardiology. V.A.E. held a BHF Clinical PhD Studentship. W.P.C. holds an MRC PhD studentship. A.V.-P. is supported by MRC career establishment award and Wellcome Trust Integrative Physiology Program. J.K.S. is a BBSRC David Phillips Research Fellow. P.A.C. was funded by Diabetes U.K.

## Glossary

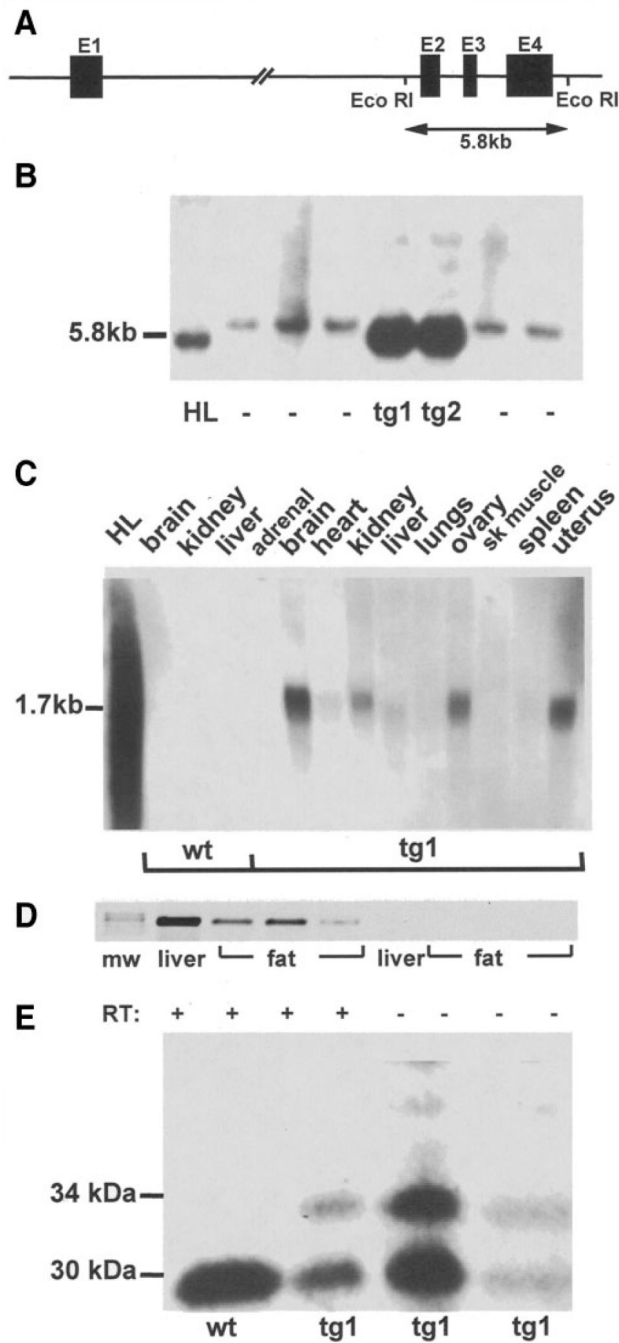
<b>BBSRC</b>	Biotechnology and Biological Sciences Research Council
<b>BHF</b>	British Heart Foundation
<b>GTT</b>	glucose tolerance test
<b>IBMX</b>	isobutylmethylxanthine
<b>IGFBP</b>	IGF-binding protein
<b>MRC</b>	Medical Research Council
<b>MRI</b>	magnetic resonance imaging
<b>PPAR<math>\gamma</math></b>	peroxisome proliferator-activated receptor $\gamma$

## REFERENCES

1. Flegal KM, Carroll MD, Ogden CL, Johnson CL. Prevalence and trends in obesity among US adults, 1999-2000. *JAMA*. 2002; 288:1723-1727. [PubMed: 12365955]
2. Fontaine KR, Redden DT, Wang C, Westfall AO, Allison DB. Years of life lost due to obesity. *JAMA*. 2003; 289:187-193. [PubMed: 12517229]
3. Gregoire FM, Smas CM, Sul HS. Understanding adipocyte differentiation. *Physiol Rev*. 1998; 78:783-809. [PubMed: 9674695]
4. Hausman DB, DiGirolamo M, Bartness TJ, Hausman GJ, Martin RJ. The biology of white adipocyte proliferation. *Obes Rev*. 2001; 2:239-254. [PubMed: 12119995]
5. Schmidt W, Poll-Jordan G, Loffler G. Adipose conversion of 3T3-L1 cells in a serum-free culture system depends on epidermal growth factor, insulin-like growth factor I, corticosterone, and cyclic AMP. *J Biol Chem*. 1990; 265:15489-15495. [PubMed: 1697591]
6. Smith PJ, Wise LS, Berkowitz R, Wan C, Rubin CS. Insulin-like growth factor-I is an essential regulator of the differentiation of 3T3-L1 adipocytes. *J Biol Chem*. 1988; 263:9402-9408. [PubMed: 2967822]
7. Deslex S, Negrel R, Ailhaud G. Development of a chemically defined serum-free medium for differentiation of rat adipose precursor cells. *Exp Cell Res*. 1987; 168:15-30. [PubMed: 3536540]

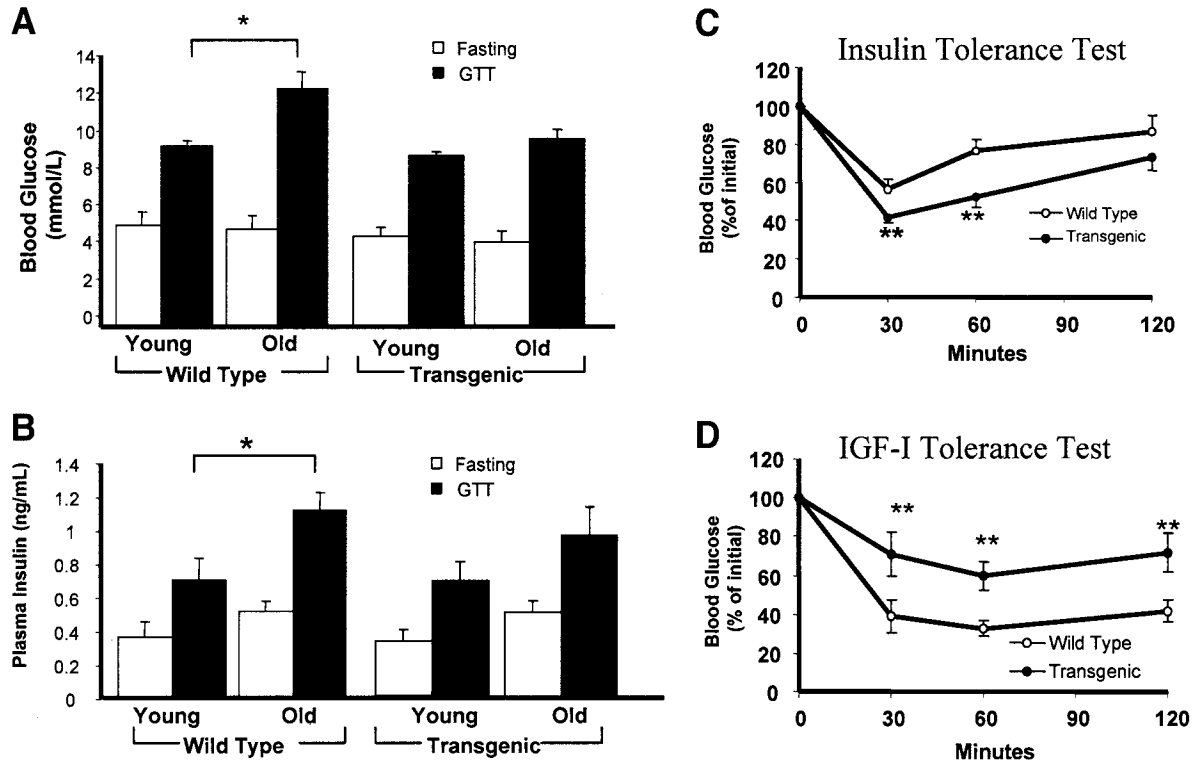
8. Nougues J, Reyne Y, Barenton B, Chery T, Garandel V, Soriano J. Differentiation of adipocyte precursors in a serum-free medium is influenced by glucocorticoids and endogenously produced insulin-like growth factor-I. *Int J Obes Relat Metab Disord*. 1993; 17:159–167. [PubMed: 7681811]
9. Ramsay TG, White ME, Wolverson CK. Insulin-like growth factor 1 induction of differentiation of porcine preadipocytes. *J Anim Sci*. 1989; 67:2452–2459. [PubMed: 2599985]
10. Kelley KM, Oh Y, Gargosky SE, Gucev Z, Matsumoto T, Hwa V, Ng L, Simpson DM, Rosenfeld RG. Insulin-like growth factor-binding proteins (IGFBPs) and their regulatory dynamics. *Int J Biochem Cell Biol*. 1996; 28:619–637. [PubMed: 8673727]
11. Firth SM, Baxter RC. Cellular actions of the insulin-like growth factor binding proteins. *Endocr Rev*. 2002; 23:824–854. [PubMed: 12466191]
12. Crossey PA, Jones JS, Miell JP. Dysregulation of the insulin/IGF binding protein-1 axis in transgenic mice is associated with hyperinsulinemia and glucose intolerance. *Diabetes*. 2000; 49:457–465. [PubMed: 10868969]
13. Crossey PA, Pillai CC, Miell JP. Altered placental development and intrauterine growth restriction in IGF binding protein-1 transgenic mice. *J Clin Invest*. 2002; 110:411–418. [PubMed: 12163461]
14. Wheatcroft SB, Kearney MT, Shah AM, Grieve DJ, Williams IL, Miell JP, Crossey PA. Vascular endothelial function and blood pressure homeostasis in mice overexpressing IGF binding protein-1. *Diabetes*. 2003; 52:2075–2082. [PubMed: 12882925]
15. Siddals KW, Westwood M, Gibson JM, White A. IGF-binding protein-1 inhibits IGF effects on adipocyte function: implications for insulin-like actions at the adipocyte. *J Endocrinol*. 2002; 174:289–297. [PubMed: 12176668]
16. Rajkumar K, Modric T, Murphy LJ. Impaired adipogenesis in insulin-like growth factor binding protein-1 transgenic mice. *J Endocrinol*. 1999; 162:457–465. [PubMed: 10467238]
17. Boney CM, Moats-Staats BM, Stiles AD, D'Ercole AJ. Expression of insulin-like growth factor-I (IGF-I) and IGF-binding proteins during adipogenesis. *Endocrinology*. 1994; 135:1863–1868. [PubMed: 7525256]
18. Frystyk J, Skjaerbaek C, Vestbo E, Fisker S, Orskov H. Circulating levels of free insulin-like growth factors in obese subjects: the impact of type 2 diabetes. *Diabetes Metab Res Rev*. 1999; 15:314–322.
19. Ehrenborg E, Vilhelmsdotter S, Bajalica S, Larsson C, Stern I, Koch J, Brondum-Nielsen K, Luthman H. Structure and localization of the human insulin-like growth factor-binding protein 2 gene. *Biochem Biophys Res Commun*. 1991; 176:1250–1255. [PubMed: 1710112]
20. Wheatcroft SB, Shah AM, Li JM, Duncan E, Noronha BT, Crossey PA, Kearney MT. Preserved glucoregulation but attenuation of the vascular actions of insulin in mice heterozygous for knockout of the insulin receptor. *Diabetes*. 2004; 53:2645–2652. [PubMed: 15448096]
21. Sethi JK, Xu H, Uysal KT, Wiesbrock SM, Scheja L, Hotamisligil GS. Characterisation of receptor-specific TNF $\alpha$  functions in adipocyte cell lines lacking type 1 and 2 TNF receptors. *FEBS Lett*. 2000; 469:77–82. [PubMed: 10708760]
22. Jitrapakdee S, Slawik M, Medina-Gomez G, Campbell M, Wallace JC, Sethi JK, O'Rahilly S, Vidal-Puig AJ. The peroxisome proliferator-activated receptor- $\gamma$  regulates murine pyruvate carboxylase gene expression in vivo and in vitro. *J Biol Chem*. 2005; 280:27466–27476. [PubMed: 15917242]
23. Prins JB, O'Rahilly S. Regulation of adipose cell number in man. *Clin Sci (Lond)*. 1997; 92:3–11. [PubMed: 9038586]
24. Yakar S, Wu Y, Setser J, Rosen CJ. The role of circulating IGF-I: lessons from human and animal models. *Endocrine*. 2002; 19:239–248. [PubMed: 12624423]
25. Doglio A, Dani C, Fredrikson G, Grimaldi P, Ailhaud G. Acute regulation of insulin-like growth factor-I gene expression by growth hormone during adipose cell differentiation. *EMBO J*. 1987; 6:4011–4016. [PubMed: 3443099]
26. O'Brien SF, Russell JC, Davidge ST. Modulation of vasomotion in resistance arteries of JCR:LA-cp rats: a model of insulin resistance. *Can J Physiol Pharmacol*. 1999; 77:71–74. [PubMed: 10535669]

27. Liu JP, Baker J, Perkins AS, Robertson EJ, Efstratiadis A. Mice carrying null mutations of the genes encoding insulin-like growth factor I (Igf-1) and type 1 IGF receptor (Igf1r). *Cell*. 1993; 75:59–72. [PubMed: 8402901]
28. Yakar S, Liu JL, Stannard B, Butler A, Accili D, Sauer B, LeRoith D. Normal growth and development in the absence of hepatic insulin-like growth factor I. *Proc Natl Acad Sci U S A*. 1999; 96:7324–7329. [PubMed: 10377413]
29. Sjogren K, Liu JL, Blad K, Skrtic S, Vidal O, Wallenius V, LeRoith D, Tornell J, Isaksson OG, Jansson JO, Ohlsson C. Liver-derived insulin-like growth factor I (IGF-I) is the principal source of IGF-I in blood but is not required for postnatal body growth in mice. *Proc Natl Acad Sci USA*. 1999; 96:7088–7092. [PubMed: 10359843]
30. Sjogren K, Wallenius K, Liu JL, Bohlooly YM, Pacini G, Svensson L, Tornell J, Isaksson OG, Ahren B, Jansson JO, Ohlsson C. Liver-derived IGF-I is of importance for normal carbohydrate and lipid metabolism. *Diabetes*. 2001; 50:1539–1545. [PubMed: 11423474]
31. Duan C. Specifying the cellular responses to IGF signals: roles of IGF-binding proteins. *J Endocrinol*. 2002; 175:41–54. [PubMed: 12379489]
32. Hoeflich A, Wu M, Mohan S, Foll J, Wanke R, Froehlich T, Arnold GJ, Lahm H, Kolb HJ, Wolf E. Overexpression of insulin-like growth factor-binding protein-2 in transgenic mice reduces postnatal body weight gain. *Endocrinology*. 1999; 140:5488–5496. [PubMed: 10579311]
33. Modric T, Silha JV, Shi Z, Gui Y, Suwanichkul A, Durham SK, Powell DR, Murphy LJ. Phenotypic manifestations of insulin-like growth factor-binding protein-3 overexpression in transgenic mice. *Endocrinology*. 2001; 142:1958–1967. [PubMed: 11316761]
34. Salih DA, Tripathi G, Holding C, Szeszak TA, Gonzalez MI, Carter EJ, Cobb LJ, Eisemann JE, Pell JM. Insulin-like growth factor-binding protein 5 (Igfbp5) compromises survival, growth, muscle development, and fertility in mice. *Proc Natl Acad Sci U S A*. 2004; 101:4314–4319. [PubMed: 15010534]
35. Bienvenu G, Seurin D, Grellier P, Froment P, Baudrimont M, Monget P, Le Bouc Y, Babajko S. Insulin-like growth factor binding protein-6 transgenic mice: postnatal growth, brain development, and reproduction abnormalities. *Endocrinology*. 2004; 145:2412–2420. [PubMed: 14749353]
36. Wood TL, Rogler LE, Czick ME, Schuller AG, Pintar JE. Selective alterations in organ sizes in mice with a targeted disruption of the insulin-like growth factor binding protein-2 gene. *Mol Endocrinol*. 2000; 14:1472–1482. [PubMed: 10976924]
37. Kershaw EE, Flier JS. Adipose tissue as an endocrine organ. *J Clin Endocrinol Metab*. 2004; 89:2548–2556. [PubMed: 15181022]
38. Momin AU, Melikian N, Shah AM, Grieve DJ, Wheatcroft SB, John L, Gamel AE, Desai JB, Nelson T, Driver C, Sherwood RA, Kearney MT. Leptin is an endothelial-independent vasodilator in humans with coronary artery disease: evidence for tissue specificity of leptin resistance. *Eur Heart J*. 2006; 27:2295–2299.

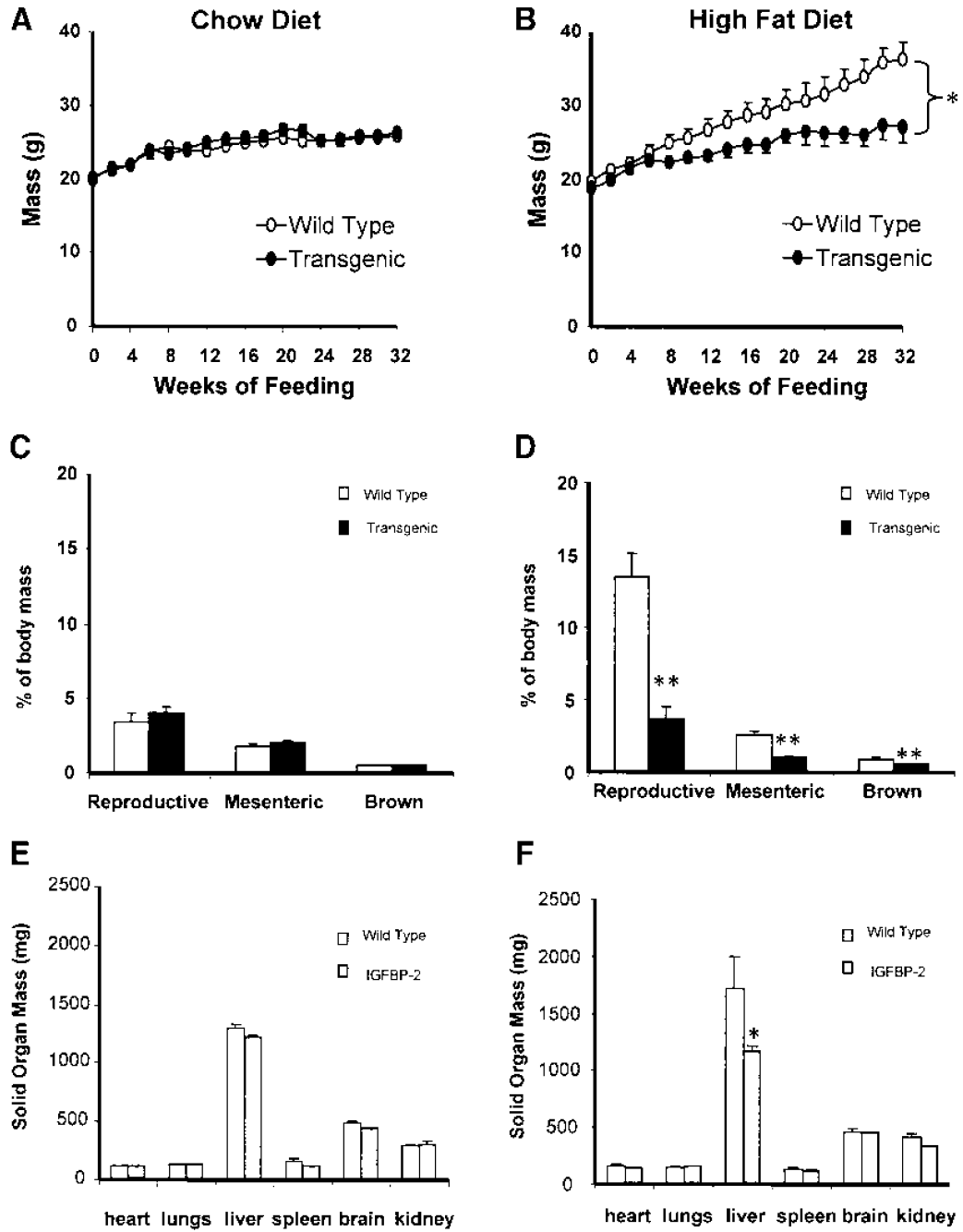
**FIG. 1.**

Generation of transgenic mice overexpressing IGFBP-2. **A:** Schematic diagram of the IGFBP-2 cosmid clone chBP2:4. Exons (1-4) are represented by solid bars, and the positions of *EcoR*I sites are indicated. **B:** Southern blot analysis of *EcoR*I-digested DNA from two lines of founder mice (tg1 and tg2) showing the characteristic 5.8-kb bands from the human IGFBP-2 gene. Other lanes contain DNA from nontransgenic mice (-) or human liver (HL). **C:** Northern analysis of tissues from wild-type (wt) and transgenic (tg1) mice probed with human IGFBP-2 cDNA. HL, RNA from human liver. **D:** RT-PCR demonstrating human

IGFBP-2 mRNA expression in reproductive fat depots from three representative transgenic mice (mw, molecular weight marker). Liver RNA was used as a positive control. RNA samples with the reverse transcription step omitted (RT-) were used as negative controls. *E*: Representative Western ligand blot of fasting sera from wt and tg1 mice. Human IGFBP-2 (34 kDa) and murine IGFBP-2 (30 kDa) are indicated (human IGFBP-2 has 18 amino acids more than the murine protein). Analysis of mean data revealed that IGFBP-2 abundance in transgenic mice was 2.2-fold greater than wild-type mice by densitometry ( $P < 0.05$ ,  $n = 12$  per group).

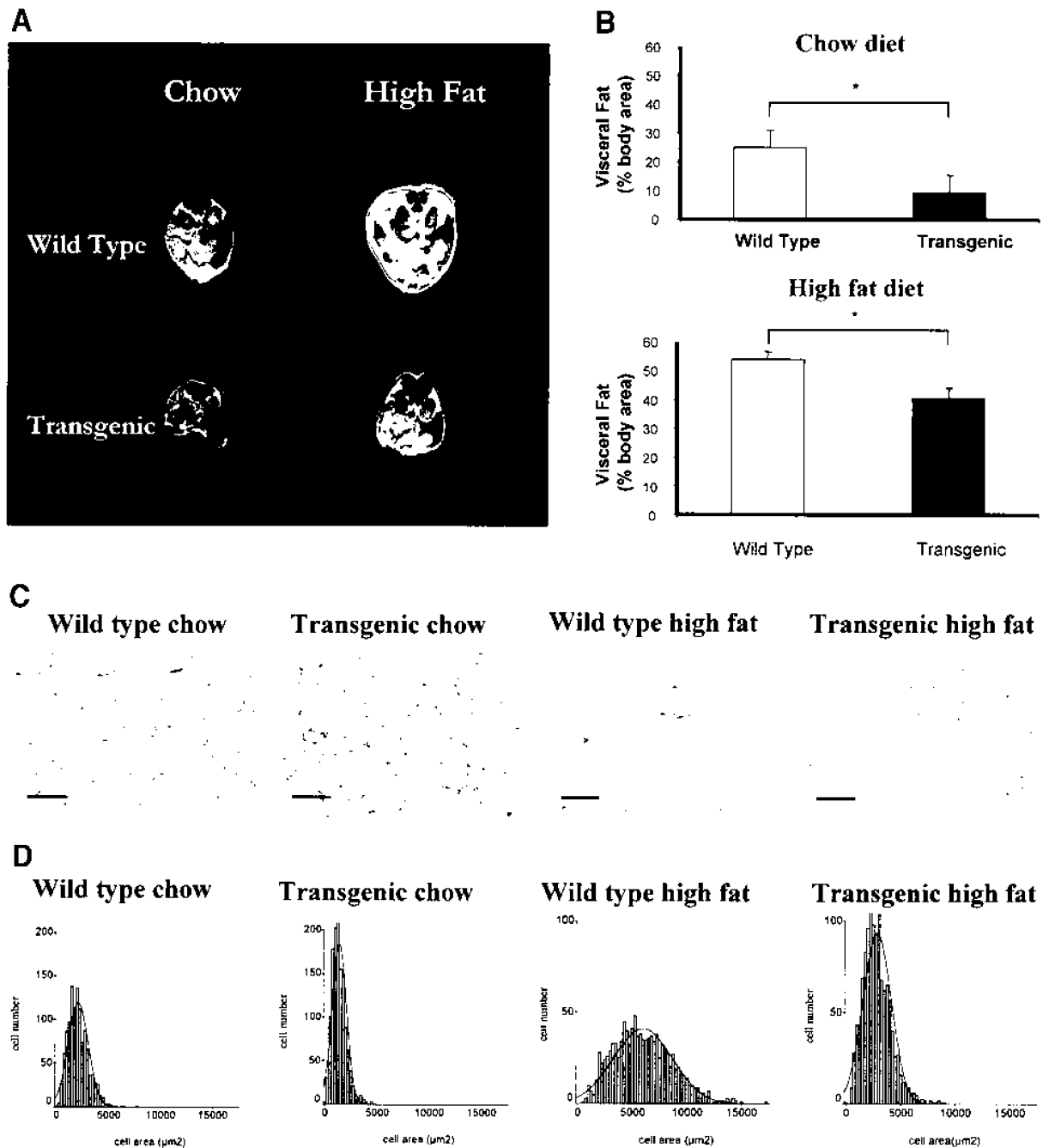
**FIG. 2.**

Age-related changes in metabolic homeostasis in wild-type and IGFBP-2 transgenic mice. *A* and *B*: Blood glucose and plasma insulin concentrations were measured after an overnight fast and 30 min after a glucose challenge (1 mg/g i.p.) in mice 8 weeks (young) and 40 weeks (old) of age. *C* and *D*: Insulin and IGF-I tolerance tests were carried out in 40-week-old mice; blood glucose levels were measured at intervals after the intraperitoneal injection of insulin (0.5 IU/kg) or IGF-I (0.2 µg/g). \* $P < 0.05$ , \*\* $P < 0.01$ ,  $n = 8-12$  per group.

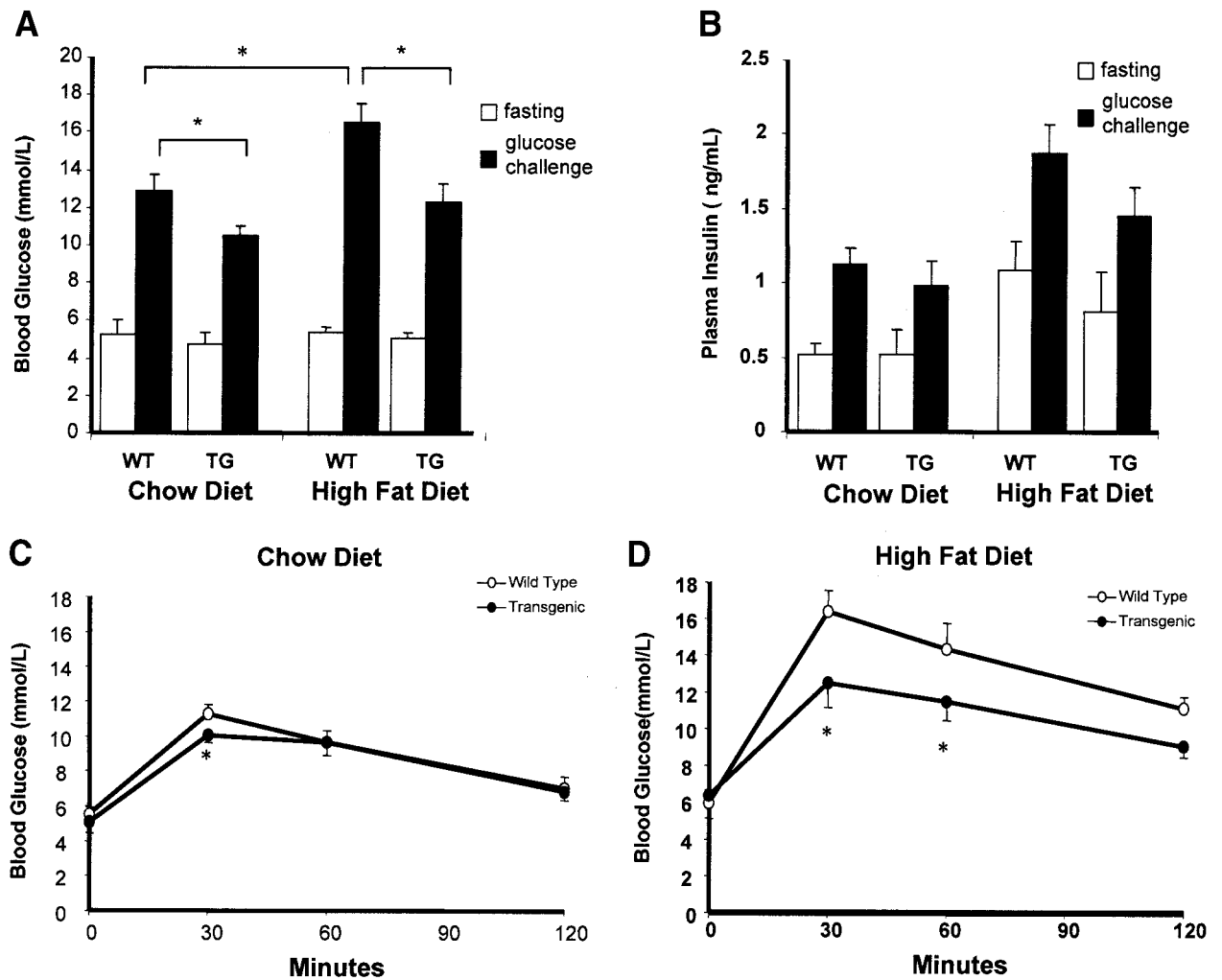


**FIG. 3.** Body mass and organ mass in response to high-fat feeding in wild-type and IGFBP-2 transgenic mice. *A* and *B*: Body mass was assessed in response to feeding standard chow or a high-fat diet for 32 weeks. *C* and *D*: Adipose tissue depot mass was measured postmortem after 32 weeks of feeding. *E* and *F*: Solid organ mass was measured postmortem after 32 weeks of feeding. \**P* < 0.05, \*\**P* < 0.01, *n* = 8–12 per group.

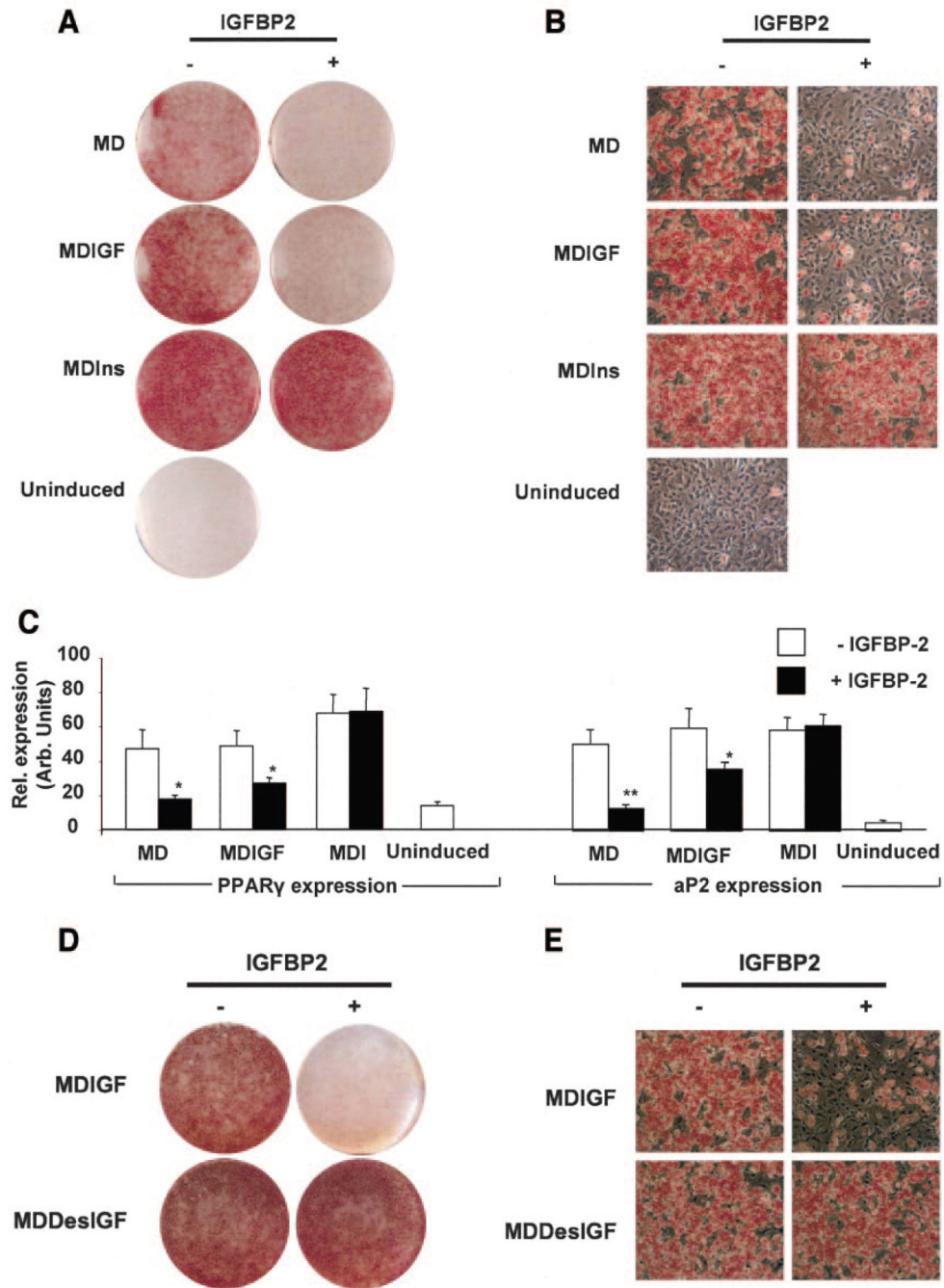


**FIG. 4.**

Changes in adiposity in response to high-fat feeding in wild-type and IGFBP-2 transgenic mice. *A* and *B*: Visceral fat was assessed by MRI in mice receiving chow or high-fat diet for 32 weeks ( $n = 3$ ). *C*: Representative sections of perigonadal fat after 32 weeks of feeding (initial magnification  $\times 10$ ; bar =  $50 \mu\text{m}$ ). *D*: Adipocyte area in histological sections of perigonadal fat after 32 weeks of feeding.  $*P < 0.05$ ,  $n = 6$  per group.

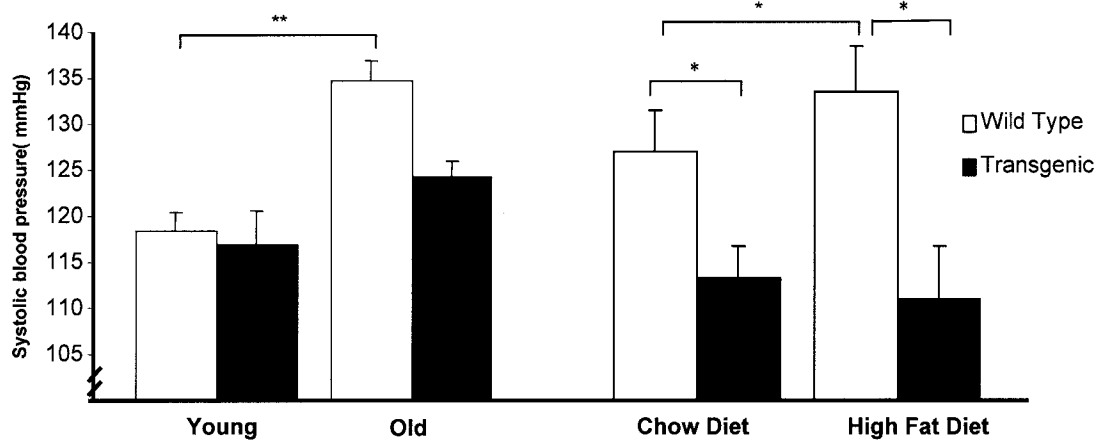
**FIG. 5.**

Changes in glucoregulation in response to high-fat feeding in wild-type (WT) and IGFBP-2 transgenic (TG) mice. *A* and *B*: Blood glucose and plasma insulin concentrations were measured after an overnight fast and 30 min after a glucose challenge in wild-type and transgenic mice receiving chow or high-fat diet for 32 weeks. *C* and *D*: Insulin-tolerance test. Blood glucose levels were measured at intervals after the intraperitoneal injection of insulin (0.5 IU/kg) after 32 weeks of feeding. \* $P < 0.05$ ,  $n = 8-12$ .



**FIG. 6.** IGFBP-2 impairs differentiation of 3T3-L1 preadipocytes. 3T3-L1 preadipocytes were induced for 2 days with either differentiation medium alone (uninduced) or differentiation medium containing either isobutylmethylxanthine (IBMX) and dexamethasone (MD); or IBMX, dexamethasone, and insulin (MDI); or IBMX, dexamethasone, and hIGF-I (MDIGF). The subsequent 2-day treatment involved the same induction cocktails minus IBMX and dexamethasone. IGFBP-2 treatment was maintained for the first 4 days of differentiation. Differentiation was terminated on day 8 after induction. *A* and *B*:

Macroscopic and microscopic views of oil red O–stained monolayers, respectively. *C*: Gene expression levels of PPAR $\gamma$  and aP2, respectively, after normalization with 18S levels. *D* and *E*: Macroscopic and microscopic views of oil red O–stained 3T3-L1 preadipocytes induced with IBMX, dexamethasone, and either hIGF-I (MDIGF) or hDes (1–3)IGF-I (MDDesIGF). Data represent means  $\pm$  SE of at least three independent experiments. Two-tailed, two sample, equal variance Student's *t* test were used to assess statistical significance. \**P* < 0.05, \*\**P* < 0.01.

**FIG. 7.**

Systolic blood pressure measured by tail-cuff plethysmography in conscious, restrained animals at 8 weeks of age (young), 40 weeks of age (old), and after feeding a chow diet or high-fat diet for 32 weeks. \* $P < 0.05$ , \*\* $P < 0.001$ ,  $n = 8-12$  per group.

**TABLE 1**

## Glucoregulation in IGFBP-2 transgenic mice

	Wild type	tg1	tg2
Blood glucose (mmol/l)			
Fasting	6.1 ± 0.8	5.8 ± 0.4	6.3 ± 0.7
Nonfasting	13.6 ± 1.1	11.1 ± 0.8*	10.4 ± 0.9*
Plasma insulin (ng/ml)			
Fasting	0.16 ± 0.01	0.15 ± 0.01	0.13 ± 0.01
Nonfasting	0.88 ± 0.12	0.71 ± 0.08	0.67 ± 0.09

Data are means ± SE from 4- to 6-month-old animals.

\*  $P < 0.05$  compared with wild type.